npj | Materials Degradation

www.nature.com/npjmatdeg

REVIEW ARTICLE OPEN

A review of plant extracts as green corrosion inhibitors for CO_2 corrosion of carbon steel

Basit Raza Fazal[1], Thomas Becker[2], Brian Kinsella[1] and Katerina Lepkova[1]✉

The use of corrosion inhibitors is a cost-effective corrosion mitigation strategy for carbon steel. There is an increased focus on developing and using low-cost, biodegradable and environmentally friendly inhibitor formulations. Plant-based extracts have been evaluated in many studies using a multitude of electrochemical methods and characterisation techniques. Although plant extracts appear as promising alternatives for commercially synthesised inhibitor formulations, a significant amount of optimisation is required. The majority of the research on plant extracts does not elucidate the effect of other synergistic combinations in commercial inhibitor formulations. Therefore, further development of plant extracts as corrosion inhibitors is of significant interest.

npj Materials Degradation (2022)6:5 ; https://doi.org/10.1038/s41529-021-00201-5

INTRODUCTION

Carbon steel is extensively used in the oil and gas industry, and due to its mechanical properties and low cost, is the preferred material for pipeline construction. Owing mainly to their much higher costs, it is not normally feasible to replace carbon steel with corrosion resistant alloys in large oil and gas trunklines. However, carbon steel is highly susceptible to corrosion. The presence of CO_2, H_2S and organic acids (acetic acid, propionic acid and formic acid) is one of the leading causes of corrosion in oil and gas production that can instigate localised or pitting corrosion[1]. This review presents an analysis of so-called plant-extract-based green corrosion inhibitors that have been investigated to mitigate CO_2 corrosion. The review is extended to also include plant-extract-based green corrosion inhibitors that were studied for their efficiency to prevent strong acid corrosion by HCl and H_2SO_4 since such products are expected to also prevent weak acid corrosion from CO_2.

CO_2 corrosion

The problem of sweet corrosion arises from the fact that CO_2 is soluble in the water that comes to the surface with production fluid, and results in the formation of carbonic acid (H_2CO_3) that, although being a weak acid, is still extremely corrosive for carbon steel. The literature identifies iron carbonate ($FeCO_3$) as the main corrosion product formed at carbon steel under CO_2 corrosive environments. The following cathodic mechanism of CO_2 corrosion has been proposed[2–4]:

$$CO_{2(g)} \rightleftharpoons CO_{2(aq\cdot)} \quad (1)$$

$$CO_{2(aq\cdot)} + H_2O_{(l)} \rightleftharpoons H_2CO_3 \rightleftharpoons H^+ + HCO_3^- \quad (2)$$

$$2H^+ + 2e^- \rightleftharpoons H_2 \quad (3)$$

$$2H_2CO_3 + 2e^- \rightleftharpoons 2HCO_3^- + H_2 \quad (4)$$

Most of the dissolved carbon dioxide is present as $CO_{2\ (aq\cdot)}$ and only about 0.2% is present as carbonic acid (Eq. 1)[5]. Reduction of protons together with the direct reduction of associated carbonic acid was the commonly accepted cathodic mechanism until challenged by Remita et al.[6]. The authors proposed that the reduction of protons (Eq. 3) is the only cathodic reaction and that the equilibrium reaction of H_2CO_3 (Eq. 4) only serves to supply more hydrogen ions. This mechanism has become known as the 'buffer effect mechanism'[6]. Experimental work conducted by other authors also supported the buffer effect mechanism[7]. There is an agreement in literature[5,8–10] that for temperatures below 50–60 °C, the rate controlling step for cathodic reaction kinetics is the hydration of carbon dioxide to carbonic acid. It was shown by Nešić[5] that at a given temperature, dissolved CO_2 is a function of pCO_2 according to Henry's law[11,12], and the concentration of H_2CO_3 is independent of solution pH and proportional to the hydration constant K_{Hyd}[5], as illustrated in Fig. 1. In contrast, bicarbonate and carbonate concentrations are a function of pH[5].

Iron dissolution is the primary anodic reaction to balance the cathodic reactions:

$$Fe_{(s)} \rightarrow Fe^{2+} + 2e^- \quad (5)$$

Bockris et al.[13] proposed the following anodic dissolution mechanism for iron in strong acids, which is often accepted to apply in saturated CO_2 solutions.

Iron combines with water according to the following equation (Eq. 6):

$$Fe_{(s)} + OH^-_{(l)} \leftrightarrow FeOH_{ads} + e^- \quad (6)$$

The adsorbed intermediate product oxidises according to the following reactions (Eqs. 7 and 8):

$$FeOH_{ads} \leftrightarrow FeOH^+ + e^- \quad (7)$$

$$FeOH^+ \leftrightarrow Fe^{2+} + OH^- \quad (8)$$

Bockris et al.[13] suggested the anodic dissolution of iron was a pH dependent process, while it was concluded by Nešić in a separate study that the pH dependency of this anodic dissolution process decreased significantly at pH > 4[10]. The anodic dissolution of iron at pH > 4 was found to be affected by the CO_2 concentration[8,9].

The complete reaction at carbon steel in a CO_2-saturated aqueous solution results in the formation of iron carbonate and the evolution of hydrogen gas (Eq. 9). Iron carbonate can

[1]Curtin Corrosion Centre, WA School of Mines: Minerals, Energy and Chemical Engineering, Curtin University, Bentley, WA, Australia. [2]School of Molecular and Life Sciences, Curtin University, Bentley, WA, Australia. ✉email: k.lepkova@curtin.edu.au

Published in partnership with CSCP and USTB

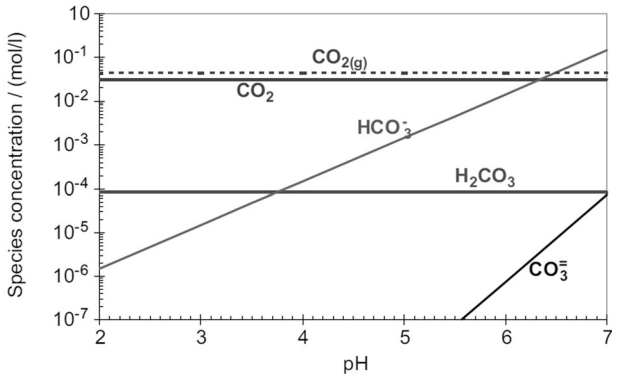

Fig. 1 Calculated carbonic species concentrations as function of pH for a CO_2-saturated aqueous solution; $pCO_2 = 1$ bar, 25 °C, 1 wt % NaCl[5]. Republished with permission from ref. [5]. Copyright 2011, John Wiley & Sons – Books.

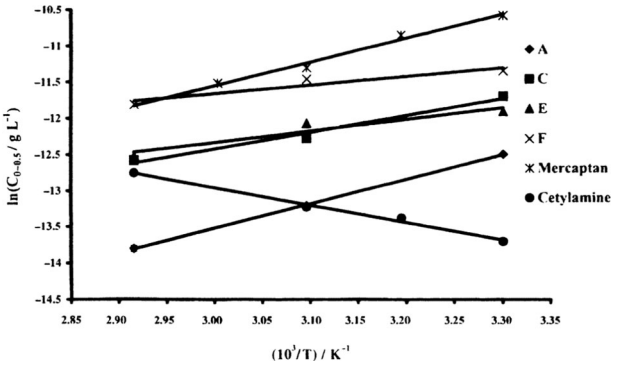

Fig. 2 Van't Hoff plots for inhibitors. A = fatty acid amine inhibitor, C = imidazoline/ester inhibitor, E = amine based fatty acid inhibitor and F = quaternary amine inhibitor[25]. Reprinted from ref. [25] with permission of Springer Nature. Springer Nature 2001.

precipitate if scaling conditions exist that are favoured by high temperature and high pH.

$$Fe_{(s)} + CO_{2(g)} + H_2O_{(l)} \rightarrow Fe^{2+} + CO_3^{2-} + H_{2(g)} \quad (9)$$

The corrosion rate in the absence of an inhibitor depends on various factors. In the absence of an inhibitor, the water chemistry and temperature determine the formation and the protectiveness of the iron carbonate scale. Iron carbonate scale precipitated at temperatures between 40 and 60 °C was found to be loose and porous, consequently leading to higher corrosion rates[10,14,15]. However, the solubility of the iron carbonate scale decreased at high pH (pH > 6.5)[16] and high temperatures ($T \geq 80$ °C) imparting slightly better corrosion resistance[17–19]. In the absence of an inhibitor, the corrosion rate was also found to increase with increasing partial pressure of CO_2 gas[3,20–22]. An increase in flow rate was also found to increase the corrosion rate in the absence of inhibitors and non-scaling conditions (pH < 6, $T < 60$ °C); however, the effect of flow rate became insignificant when scaling conditions (pH ≥ 6, $T \geq 60$ °C) were achieved[3,10].

Corrosion inhibitors

Amongst the various ways of mitigating corrosion (coating, alloying, etc.), the use of chemical compounds known as corrosion inhibitors is one of the most cost-effective corrosion mitigation strategies for carbon steel. A corrosion inhibitor is typically used in small concentrations and essentially minimises the corrosion rate by inhibiting the reaction of metal with its environment. Hence, the use of inhibitors allows low-cost carbon steel to be used as a structural material. An ideal inhibitor is described as one which is composed of low cost, abundant and environmentally friendly constituents[23].

A synthetic commercial corrosion inhibitor formulation applied in oil and gas production usually contains one or more of the following: quaternary ammonium salts (called quaternary amines in oilfield parlance), fatty acids, fatty amines/diamines, imidazolines, and oxygen, sulfur or phosphorus containing compounds.

The polar functional groups, commonly present in aforementioned compounds, are regarded as main instigators for the adsorption process. The adsorption behaviour of an organic inhibitor is in turn governed by physiochemical properties of the molecule such as the electronic density of donor atoms[24]. Durnie et al. conducted various in-depth studies on the adsorption of several different commercial carbon dioxide corrosion inhibitor formulations using quantum mechanical calculations to show that a range of molecular parameters determined the thermodynamic adsorption properties of carbon dioxide corrosion inhibitors[25–27]. Durnie et al.[25] used the Van't Hoff plots illustrated in Fig. 2[25] to show that inhibitors exhibited either an endothermic or positive enthalpy, or an exothermic (negative) enthalpy of adsorption. In the case of the inhibitors shown in Fig. 2, all except the cetylamine demonstrate endothermic or positive enthalpy of adsorption. Their efficiency improved at increased temperature with less inhibitor required to produce the same level of protection as the temperature increased[25].

Organic inhibitor molecules can adsorb on the metal surface via either:

(i) hydrolysis of organic compounds, for example, anhydrides (hexadecylsuccinic anhydride) hydrolysing to form fatty dicarboxylic acids, leading to the formation of insoluble ferrous salts on the metal surface, or
(ii) donor–acceptor exchanges between the vacant d-orbital of iron atoms and π-electrons of aromatic rings in inhibitor molecules, or
(iii) interactions between unshared electron pairs of the oxygen/nitrogen/sulfur atoms and vacant d-orbital of iron atoms, or
(iv) interactions between d-orbital electrons of iron atoms and the vacant orbital of the oxygen/nitrogen/sulfur atoms.

Adsorption of inhibitor molecules usually takes place on active surface sites on the metal. The higher electron density on the functional groups facilitates greater adsorption through easier bond formation, and consequently, provides higher inhibition.

Many synthetic organic inhibitors are toxic and thus pose a great risk to the environment and human health. For example, a few researchers have tested zinc cations as synergists with plant extracts for inhibiting steel corrosion in aerated neutral chloride solutions[28,29]. However, zinc, being a heavy metal, could lead to environmental hazards if disposed of in excessive quantities. Therefore, the need to find eco-friendly substitutes with similarly high efficiencies has driven many researchers to investigate different plant extracts in various environments.

Plant extracts as corrosion inhibitors

Plants in their entirety are composed of various types of chemicals and out of those, the non-nutritive components responsible for a plant's smell, taste and colour are called 'phytochemicals'. Phytochemicals can be divided into different classes such as terpenoids, polyphenols and organic acids and these groups can further be classified, for example, as shown in Table 1. Molecular structures of some of these phytochemicals are given in Fig. 3. Phytochemicals typically have electronic structures that can closely resemble those of conventional synthetic organic corrosion inhibitors. Hence, it is accepted that many compounds can provide corrosion resistance to steel in corrosive media[30–32]. The non-toxic nature of the majority of the plants and their extracts make them a viable replacement option for toxic organic

Table 1. Example of phytochemicals classification.

Phytochemicals						
Phenolic compounds	Terpenoids	Organic acids lipids and related compounds	Nitrogen compounds	Organosulfur compounds	Sugar and their derivatives	Macromolecules
• Flavonoid pigment • Phenols and phenolic acids • Tannins	• Carotenoids • Triterpenoids • Saponins	• Fatty acids	• Amino acids • Amines • Alkaloids	• Indoles and thiosulfonates • Isothiocyanates	• Monosaccharides • Oligosaccharides	• Proteins • Polysaccharides

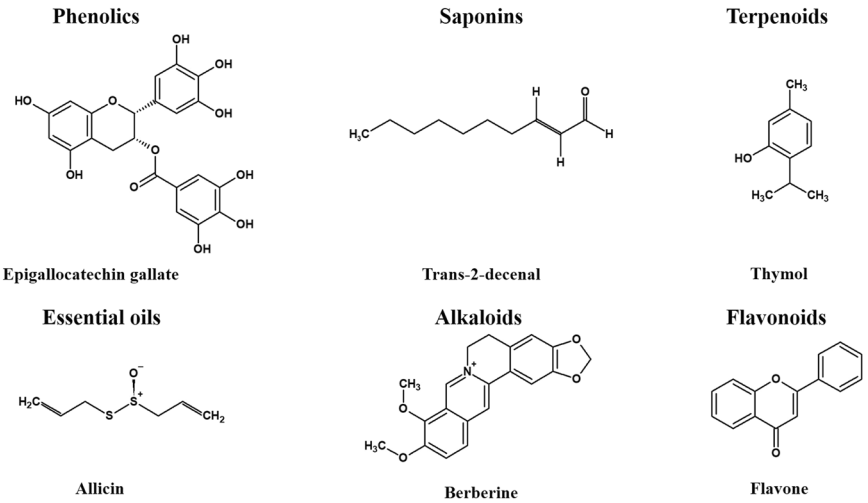

Fig. 3 Chemical structure of some phytochemicals[36]. Republished with permission from ref. [36]. Copyright 2014, CC-BY Creative Commons.

inhibitors. They are also attractive because of their biodegradable nature that makes their disposal simpler. The extraction process is also relatively simple and economical. Environmentally friendly corrosion inhibitors can be extracted from various parts of a plant such as fruit, leaves, bark, roots, seeds or peels.

The inhibitive properties of a plant extract can generally be attributed to the mix of phytochemicals in it, having various functional groups capable of adsorbing on a metal surface. However, it is because of their complex composition that a full understanding of the corrosion inhibition mechanism of biomass extracts is yet to be determined. It is difficult to study the individual and/or combined interactions of organic species with the metal surface without isolating the active constituents of any biomass extract[33–35].

Environmental regulations

The application of plant extracts as green inhibitors in industrial scenarios requires conformation to the strict regulations prepared by different bodies based on their specific geographical locations. The Oslo and Paris Commission[36,37] describes an ideal green inhibitor as one that is non-toxic, readily biodegradable and showing no bioaccumulation. The following schemes exist that outline the criteria for evaluating green corrosion inhibitors:

- The Oslo and Paris Commission, formerly known as Paris Commission (PARCOM)[37].
- The North Sea (UK, Norway, Denmark, The Netherlands) set up under Paris Commission[37].
- United States Scheme[37].
- Harmonized Mandatory Control System[37].

For instance, the principal criteria for inhibitor acceptance as per the North Sea (UK, Norway, Denmark, The Netherlands) scheme are as follows[36,37]:

- Biodegradability: >60% in 28 days.
- Marine toxicity: effective concentration, 50% (EC50)/lethal concentration, 50% (LC50) >10 mg L^{-1} to North Sea species.
- Bioaccumulation: logarithm of the ratio of octanol to water partition coefficient (log(*Po/w*)) < 3.

Evaluation techniques

Analytical techniques to evaluate the performance of corrosion inhibitors are based on electrochemical and weight loss measurements. The electrochemical methods usually employ linear polarisation resistance (LPR), electrochemical impedance spectroscopy (EIS) and Tafel extrapolation techniques, or a combination of these methods. Electrochemical noise (ECN) has been used in only a few studies[38,39]. This is surprising since it has the potential for detecting localised forms of corrosion[19,40,41], which is an important aspect in the evaluation of corrosion inhibitors. A problem using ECN is that experimental issues such as drift and asymmetry complicate the way how the current and voltage noise signals are processed to detect localised corrosion events. These advances in signal processing may lead to more researchers using ECN to evaluate inhibitor performance[19,41].

The majority of electrochemical evaluations of inhibitor performance are conducted in a conventional three electrode glass cell. The LPR technique records the current response of the metallic specimen when very small voltage variations are applied to it both in the positive and negative direction of its corrosion potential. Polarisation resistance, the ratio of voltage to current, is then used to calculate the corrosion rate by application in the Stern–Geary equation. EIS is another useful technique that captures the response of a nonlinear electrochemical system as a function of applied potential and provides information on the metal/electrolyte interface. Tafel extrapolation plots depict any changes in corrosion mechanism through changes in the Tafel slope and direct measurement of the corrosion current is obtained

without the application of the Stern–Geary equation. The nature of an inhibitor may be determined by observing the displacement in the value of corrosion potential (E_{corr}). If the difference between the value of E_{corr} for the inhibited with respect to the uninhibited specimen is at least +85 mV, the inhibitor is classified as anodic while a difference of −85 mV with respect to uninhibited specimen suggests the inhibitor is cathodic[42,43]. However, the inhibitor is classified as a mixed type if the displacement in either anodic or cathodic direction is less than 85 mV.

In addition to the calculation of corrosion rate, surface coverage can also be determined using data obtained from common electrochemical techniques. An adsorption isotherm is then typically used to relate the concentration of inhibitor in solution to the amount of inhibitor adsorbed on the surface. This surface coverage of the inhibitor is in turn used to calculate the release of energy when adsorbate molecules separate from the surface. When the release of energy is in the range of 8–25 kJ mol^{-1} due to adsorption, the phenomenon is known as physisorption. On the other hand, chemisorption takes place when much higher energy, typically greater than 40 kJ mol^{-1} or comparable to chemical bonding, is released. Any release of energy between 25 and 40 kJ mol^{-1} is indicative of physisorption and partial chemisorption. Evaluation of such adsorption isotherms is hence believed to provide an insight into the inhibition mechanism[44,45]. Therefore, the majority of researchers have fitted their inhibitor performance measurements to adsorption isotherms to determine fundamental thermodynamic parameters. The data have been fitted to a number of isotherms, including Freundlich, Temkin and Langmuir adsorption isotherms; however, most of the researchers found Langmuir adsorption isotherm to give the best fit[46–56].

Surface characterisation is conducted on freshly polished carbon steel coupons after immersion in uninhibited and inhibited solutions. The resulting topographical images show how the addition of plant-extract-based inhibitor changes the surface roughness of the sample. Scanning electrochemical microscopy (SECM) is an in situ technique that can measure the local electrochemical behaviour at the metal/electrolyte interface. A probe tip scans across the surface and detects changes in current as a function of the distance between tip and surface resulting in topological images indicative of either a conducting or an insulating surface. In a few studies, SECM has been used to observe the electrochemical activity on metallic surfaces in the presence and absence of green inhibitors. The resulting plots can then verify the formation of an insulating layer due to inhibitor addition[46–48,57].

Scanning electron microscopy (SEM) is the most commonly used surface characterisation technique; however, some studies have also used atomic force microscopy (AFM)[58–67]. Although AFM has only been used to compare the surface roughness of the samples after immersion in blank and inhibitor-containing solutions, it is suggested that AFM is a powerful tool that can also be used to study the in situ inhibitor adsorption process as demonstrated by a few researchers[64].

Fourier-transform infrared spectroscopy (FTIR) is a non-destructive surface characterisation technique. Exposing a material to infrared (IR) light results in an IR spectrum detailing the absorbance and/or transmittance as a function of IR wavelength. An IR spectrum is an inherent characteristic of that specific material. Such IR spectra of known materials are used as a reference to identify any unknown material or detect the presence of known chemicals or compounds in or on a specimen. Hence, many researchers have conducted an ex situ FTIR analysis to detect the presence of phytochemicals on metal surface after corrosion studies[47–50,54,57,58,68]. This was achieved by comparing the IR spectra acquired from a corroded surface in a blank solution with the IR spectra obtained from the specimen that had been immersed in an inhibitor-containing solution.

Quantum chemical calculation is a theoretical chemistry approach that is used to explain the corrosion inhibition mechanisms. Using this technique, it is possible to calculate structure parameters such as energy and distribution of highest occupied molecular orbital (HOMO) and lowest unoccupied molecular orbital (LUMO), the absolute electronegativity values and the fraction of electrons (Δn) transferring from inhibitors to metal specimen. Since this technique allows to study the structure-reactivity of the different compounds present in a plant extract, many researchers prefer to employ quantum chemical computations and molecular dynamic simulations to identify and shed light on the individual interactions of active organic constituents of green inhibitor with a metallic substrate at the molecular level[48,54,59,62,63,65,69–72].

Inhibitor preparation

The plant extraction process is a solid/liquid separation procedure that consists of soaking the plant in an appropriate solvent. The approach taken by most researchers to obtain plant-based inhibitors involves washing, drying and crushing plant roots, barks, leaves or peel to a powder form. It is possible to use commercially available extract powder as well as to prepare inhibitor stock solutions[68]. The plant extract powder is subjected to the extraction process that includes the addition of an organic solvent such as ethanol or methanol and allowing the powder to soak for a long time, usually between 24 and 72 h at room temperature. The mixture is then usually refluxed and filtered to obtain the dissolved plant extracts. Green inhibitors are often obtained after heating to distil the solvent or drying the filtrate in an oven to remove the excess solvent. Concentrated extracts are then diluted to prepare inhibitor solutions of various concentrations. In one particular instance, sulfated fatty acid (SFA) inhibitors were synthesised via hydrolysis of corn oil and then using the products in a sulfating treatment[50], while another group of researchers treated the plant extract with a reducing agent to make a water-soluble inhibitor solution[73,74].

It is worth mentioning here that most studies report the inhibitor concentration in parts per million (ppm) when instead it might be beneficial to report the concentration in mol L^{-1}. However, it is difficult to report concentrations in mol L^{-1}without knowing the exact chemical composition of the plant extract. It should be noted that to be strictly correct ppm should be equivalent to mg kg^{-1} (1000 g) or micro-litres per litre (μL L^{-1}); however, the use of mg L^{-1} is often used to be equivalent to ppm since it is assumed that one litre of aqueous solution weighs 1000 g. This is, however, not strictly correct since the weight or density of water varies with the temperature and composition of dissolved ingredients.

GREEN INHIBITORS FOR CO_2-SATURATED CORROSIVE MEDIA

This section presents a summary of advances in research on plant extracts used as CO_2 corrosion inhibitors. The plant extracts in this section are ordered according to their efficiency to mitigate the relevant corrosion processes, starting with the most efficient products.

Cashew nut

Philip et al.[73,74] experimented with cashew nut shell liquid as a green corrosion inhibitor for SAE 1008 carbon steel immersed in CO_2-saturated 3% NaCl solution. All experiments evaluated the performance of the inhibitor at a concentration range from 10 to 1200 ppm. Experiments were conducted at 30 °C and at two different pH values, i.e. pH 4 and pH 6. The pH was adjusted using either sodium bicarbonate ($NaHCO_3$) or diluted hydrochloric acid (HCl)[73,74].

Cardanol was identified as the main component of cashew nut shell liquid (CNSL) that is typically obtained as a by-product during thermal processing of cashew kernel (*anacardium occidentale*). A water-soluble solution of CNSL was prepared by making an emulsion with ethanol followed by treatment with hydrazine hydrate and 0.1 M sodium hydroxide solution. Two major conclusions were drawn from the initial potentiodynamic polarisation experiments. Firstly, addition of the inhibitor was found to lower both the anodic and cathodic corrosion currents. Hence, the inhibitor was ranked as mixed-type inhibitor. Secondly, addition of the inhibitor at pH 4 shifted the corrosion potential in a nobler direction compared to the uninhibited corrosion potential, while addition of the inhibitor at pH 6 shifted the corrosion potential in an active direction with respect to the uninhibited potential. This indicated a change of corrosion mechanism of SAE 1008 carbon steel at higher pH values. At pH 4 the corrosion rate dropped from 0.640 millimetres per year (mm y^{-1}) in uninhibited solution to 0.113 mm y^{-1} in 1200 ppm inhibitor-containing solution, while at pH 6 the corrosion rate dropped from 0.299 mm y^{-1} in uninhibited solution to 0.002 mm y^{-1} in 1200 ppm inhibitor-containing solution. This corresponded to a maximum inhibition efficiency of 82% and 99% at pH 4 and pH 6, respectively, which suggested that cashew nut shell inhibitor performs better in the solutions with higher pH. Further experiments were then conducted in solutions at pH 6 and inhibitor concentrations varying from 10 to 1200 ppm were tested. Tafel curves showed that the corrosion current density decreased as inhibitor concentration increased. The corrosion current was found to decrease from 34.60 mA cm^{-2} in uninhibited solution to 2.55 mA cm^{-2} in a solution containing 300 ppm of CNSL. This corresponded to a decrease in corrosion rate from 0.4 mm y^{-1} in uninhibited solution to 0.03 mm y^{-1} in inhibitor-containing solution and indicated a maximum efficiency of 92% at an inhibitor concentration of 300 ppm. No significant drop in corrosion current was observed for further increase in inhibitor concentration. EIS results showed a continuous increase in impedance and phase angle as the inhibitor concentration was increased, which correlates to inhibitor film growth. The authors successfully used EIS data to suggest that a minimum of 8 h of immersion was required for the complete development of the inhibitor film and maximum protection of the metal surface. This immersion time was found to be independent of the inhibitor concentration as the charge transfer resistance and double-layer capacitance values became constant after 8 h of exposure.

The authors addressed the different inhibitor behaviour at two different pH values, and suggested that cardanol, a phenol, which is the primary active ingredient of the inhibitor, is a weak acid and therefore has low solubility in low pH solutions. Hence, it was concluded that a lower inhibition efficiency at pH 4 was due to the inability of the inhibitor molecules to ionise fully and consequently adsorb on the surface. Further experiments carried out at only pH 6 were aimed to understand the influence of surface charge on inhibitor adsorption mechanism. According to the literature, when the difference between corrosion potential and potential of zero charge is positive adsorption of anions is favoured and vice versa[43]. The authors used EIS to calculate the potential of zero charge and calculations conducted after EIS showed that the carbon steel surface immersed in inhibitor-containing solution at pH 6 was positively charged. Subsequently, the adsorption of inhibitor on the substrate surface was studied as a function of the applied potential. The results demonstrated that the concentration of adsorbed inhibitor on the metal surface increased as the positive charge on the surface increased[73,74].

Tridax procumbens and *chromolaena odorata*

Aribo et al.[52] tested the extracts from two different plants, *tridax procumbens* and *chromolaena odorata*, for their effectiveness in protecting UNS S31254 super austenitic stainless steel exposed to a CO_2-saturated acidising oilfield environment. The environment was simulated by mixing 4 M HCl solution and 3.5% NaCl solution in equal ratios. Both inhibitors were studied at four different concentrations (100, 200, 300 and 400 ppm). All experiments were conducted at 40 °C[52].

Chromolaena odorata is a flowering shrub that belongs to the sunflower family—*asteraceae*, while *tridax procumbens* is a common tropical weed. Phytochemical screening of the leaf extract of both inhibitors showed that *tridax procumbens* was rich in flavonoids, alkaloids, hydroxycinnamates, tannins, phytosterols, benzoic acid and lignans. Similarly, *chromolaena odorata* was found to contain tannins, steroids, terpenoids, flavonoids, phenols, saponins and glycosides. Tafel plots obtained from the individual study of the two different inhibitors showed that they suppressed anodic reactions and thus can be identified as anodic inhibitors. Tafel plots also showed that the corrosion potential shifted towards the anodic direction in both cases. The corrosion rate was observed to drop upon the addition of each inhibitor extract. At the same concentration of 100 ppm, addition of *tridax procumbens* extract reduced the corrosion rate from 18.208 mm y^{-1} in blank solution to 0.009 mm y^{-1}, while the addition of *chromolaena odorata* extract reduced the corrosion rate from 18.208 to 0.021 mm y^{-1}. These values corresponded to a maximum inhibition efficiency of 99% for both inhibitor extracts. The calculated surface coverage for both inhibitors was found to be consistent with the Langmuir adsorption isotherm[52]. It is pointed out that because stainless steel generally undergoes localised corrosion and not general corrosion, and since LPR and EIS measure only a general or uniform corrosion rate, these inhibitors are not summarised in Table 2.

Kuding

Chen et al.[47] studied the inhibitive properties of kuding leaf extract on J55 steel immersed in a CO_2-saturated 3.5% NaCl solution at room temperature. Solutions with six different inhibitor concentrations (v/v), 0.1%, 0.5%, 1%, 2%, 3% and 4% were prepared[47]. The conversion of these concentrations corresponds to 1000, 5000, 10,000, 20,000, 30,000 and 40,000 ppm.

It was reported that active constituents in kuding, a tea infusion derived from several plant species, are isoflavones, flavonols, dihydroflavonol and anthocyanidins. It was shown from potentiodynamic polarisation curves that the addition of inhibitors decreased the corrosion current density. Inhibition efficiency and surface coverage were found to increase as inhibitor concentration increased. This green inhibitor was identified as a mixed-type inhibitor since the change in corrosion potential in the absence and presence of inhibitor was less than 85 mV. The corrosion rate calculated from potentiodynamic polarisation parameters showed that it decreased from 0.418 mm y^{-1} in blank solution to 0.014 mm y^{-1} in the solution having 4% v/v (40,000 ppm) of inhibitor. This translated to maximum efficiency of 96%. Nyquist plots obtained from EIS showed a typical single capacitive loop for the sample immersed in uninhibited solution indicating a normal charge transfer controlled corrosion process while two capacitive loops were obtained in inhibitor-containing solutions indicating the presence of an inhibitor film. The diameter of both capacitive loops was also found to increase as inhibitor concentration increased. Comparison of 3D plots obtained from SECM analysis confirmed that an insulating layer was formed on the steel sample immersed in inhibited solutions. It was observed from SEM images that the addition of inhibitor resulted in smooth and less corroded surface morphology. Langmuir adsorption isotherm best fitted the experimental surface coverage data. The calculated slopes for the adsorption isotherm suggested the formation of a monolayer of inhibitor molecules on the metal surface with no interaction between adsorbed molecules[47].

Table 2. Green corrosion inhibitors for preventing CO_2 corrosion sorted based on the lowest corrosion rate obtained from polarisation parameters.

Plant extract	Steel specimen	Inhibitor concentration (at max. IE%)	Testing temperature (°C)	Uninhibited corrosion rate (mm y^{-1})	Inhibited corrosion rate (mm y^{-1})	Testing solution
Cashew nut shell liquid	SAE 1008 CS	1200 ppm	30	0.299	0.002	CO_2-saturated 3.0% NaCl (pH 6)
Kuding	J55	4 v/v % (40,000 ppm)	25	0.418	0.014	CO_2-saturated 3.5% NaCl
Olive leaf	N80	300 ppm	25	1.297	0.019	CO_2-saturated 3.0% NaCl + 0.01% $NaHCO_3$ + 0.01% $CaCO_3$
Cashew nut shell liquid	SAE 1008 CS	300 ppm	30	0.402	0.030	CO_2-saturated 3.0% NaCl (pH 6)
Jatropha curcas leaf extract	API 5L-X65	400 ppm	25	1.205	0.040	CO_2-saturated 3.5% NaCl (pH 4.7)
Olive leaf	N80	300 ppm	65	1.262	0.064	CO_2-saturated 3.0% NaCl + 0.01% $HaHCO_3$ + 0.01% $CaCO_3$
Jatropha curcas leaf extract	X65 MS	400 ppm	50	2.449	0.095	CO_2-saturated 3.5% NaCl (pH 4.7)
Sida acuta	API 5L-X65	400 ppm	25	1.162	0.112	CO_2-saturated 3.5% NaCl (pH 4.5)
Cashew nut shell liquid	SAE 1008 CS	1200 ppm	30	0.640	0.113	CO_2-saturated 3.0% NaCl (pH 4)
Coptis chinensis	L360 CS	50 ppm (+10 ppm Thiourea)	60	2.661	0.113	CO_2-saturated 3.0% NaCl
Liquorice	API 5L Grade B	3000 ppm	25	0.639	0.115	CO_2-saturated 3.5% NaCl + 0.3% $CaCl_2$ + 0.2% $MgCl_2.6H_2O$ (~pH 4.0)
Tobacco leaf	AISI 1045	132.5 ppm	–	0.330	0.121	CO_2-saturated 3.5% NaCl(pH 7)
Pomelo	N80	400 ppm	30	1.845	0.124	CO_2-saturated 3.5% NaCl (pH 4.2)
Calotropis procera	MS	200 ppm	25	2.921	0.230	CO_2-saturated 3.5% NaCl
Tobacco leaf	AISI 1045	265 ppm	–	1.774	0.244	CO_2-saturated 3.5% NaCl (pH 4)
Corn oil-derived diethanolamine sulfated fatty acid	C1018 MS	100 ppm	50	24.401	0.244	CO_2-saturated 1% NaCl (pH 5.60)
Berberine	L360 CS	100 ppm (+10 ppm Thiourea)	60	2.661	0.282	CO_2-saturated 3.0% NaCl
Calotropis procera	MS	200 ppm	40	4.463	0.325	CO_2-saturated 3.5% NaCl
Calotropis procera	MS	200 ppm	50	4.463	0.325	CO_2-saturated 3.5% NaCl
Jatropha curcas oil	A106 CS	150 ppm	Room temperature	2.24[a]	0.39[a]	CO_2-saturated 3.0% NaCl
Dimocarpus longan	API 5L	400 ppm	Ambient temperature	0.923	0.454	CO_2-saturated 1.3% NaCl + 0.09% $HaHCO_3$ + 0.74% Na_2SO_4

Olive leaf

Pustaj et al.[68] studied the corrosion behaviour of N80 carbon steel in CO_2-saturated chloride carbonate solution in the absence and presence of olive leaf extract at two different temperatures, 25 and 65 °C. The inhibitor was evaluated at three different concentrations (100, 200 and 300 mg L^{-1} equivalent to 100, 200 and 300 ppm) under dynamic conditions (300 rpm). The test solution was prepared by mixing 3% NaCl, 0.01 % $NaHCO_3$ and 0.01% $CaCO_3$[68].

The known organic components in olive leaf are oleuropein and its derivatives such as hydroxytyrosol and tyrosol, caffeic acid, p-coumaric acid, vanillic acid, vanillin, luteolin, diosmetin, rutin, luteolin-7-glucoside, apigenin-7-glucoside and diosmetin-7-glucoside[75–77]. In uninhibited solution, it was found that with increasing exposure time the polarisation resistance decreased from 268 to 211 Ω cm^2 at 25 °C, while it increased from 120 to 243 Ω cm^2 at 65 °C. This was attributed to the formation of corrosion products with better protective properties at high temperatures. The addition of inhibitor was found to drastically increase the polarisation resistance values and shift the corrosion potential towards nobler values at both temperatures. Since the difference in corrosion potential obtained in uninhibited and inhibited solutions at both temperatures was less than 85 mV, the inhibitor was identified as mixed-type inhibitor. It was found that the addition of 300 mg L^{-1} (300 ppm) of olive leaf extract after 24 h of exposure to synthetic brine reduced the corrosion rate from 1.297 to 0.019 mm y^{-1} at 25 °C and from 1.262 to 0.064 mm y^{-1} at 65 °C with inhibition efficiency of 98% and 94%, respectively. Impedance plots revealed that increased inhibitor concentration and longer exposure time resulted in larger impedance modules as compared to those obtained in uninhibited solution. A similar trend was observed at both experimental temperatures. Comparison of the surface morphology of corroded and inhibited samples showed that an inhibited sample had a compact protective layer without pores or other defects. SEM analysis also indicated that olive leaf extract had anti-scaling properties as well. FTIR absorption bands obtained after immersing the steel sample for 24 h in inhibitor-containing simulated brine showed peaks associated with functional groups present in olive leaf extract. This confirmed the formation of a protective layer on the sample immersed in inhibited solution[68].

Jatropha curcas

Mohadyaldinn and Azad[78] worked with *jatropha curcas* oil as a green corrosion inhibitor for A106 carbon steel. Tests were conducted in CO_2-saturated 3% NaCl solution at room temperature using rotating cylinder electrodes (RCEs). The inhibitor was tested at three different concentrations (50, 100 and 150 ppm) under both static and dynamic conditions[78].

LPR tests conducted under static conditions (0 rpm) showed that higher concentrations of 100 and 150 ppm resulted in

corrosion rates lower than 0.1 mm y^{-1}. LPR tests conducted under dynamic conditions (500 rpm) revealed that a concentration of only 100 ppm decreased the corrosion rate to less than 0.5 mm y^{-1} and maintained this value throughout the exposure period. When the RCE was rotating at 500 rpm, the corrosion rate was observed to be greater than 1 mm y^{-1} for 150 ppm, while the corrosion rate continuously increased from approximately 0.1 mm y^{-1} to more than 1 mm y^{-1} for 50 ppm. At a concentration of 150 ppm, increasing the rotation speed from 500 to 1500 rpm resulted in corrosion rates lower than 0.01 mm y^{-1}. The authors have not discussed the reason why increasing the rotation speed improved inhibitor performance at the same concentration of 150 ppm. Weight loss experiments were also performed and the results were used to calculate inhibition efficiency and corrosion rates. The corrosion rate calculated from weight loss experiments was found to decrease from 2.24 to 0.39 mm y^{-1} that corresponded to an inhibition efficiency of 82% for a concentration of 150 ppm[78].

In a separate study, Aribo et al.[55] evaluated *jatropha curcas* leaf extract as a green inhibitor for protecting API 5L-X65 steel. Inhibitor concentrations of 100, 200, 300 and 400 ppm were tested. Comparisons were made between results obtained at two different temperatures, 25 and 50 °C, and in two different environments, CO_2- and O_2-saturated 3.5% NaCl solution. All tests were carried out under static conditions. The measured pH of the CO_2-saturated brine was 4.7, while the pH for aerated brine was 6.5[55].

Phytochemical screening showed the extract to be primarily composed of saponins, and smaller quantities of tannins, flavonoids, alkanoids, calcium oxalate and terpenoids. Tafel plots of the mild steel sample in CO_2 and aerated corrosive media showed that anodic inhibition was predominant at both temperatures. For the CO_2-saturated salt solution, the corrosion rate decreased as inhibitor concentration increased. Polarisation curves and open circuit potentials were used together to show that the corrosion potential difference between uninhibited and inhibited states was less than 85 mV and thus the inhibitor was identified as mixed-type inhibitor. Calculation of inhibition efficiency revealed that the green inhibitor had better performance in CO_2 environment. Inhibition efficiency of more than 95% was reported at both temperatures in sweet conditions. At 400 ppm inhibitor concentration, the corrosion current dropped from 103.72 µA cm^{-2} ($CR = 1.205$ mm y^{-1}) to 3.48 µA cm^{-2} ($CR = 0.040$ mm y^{-1}) at 25 °C, while the corrosion current dropped from 210.76 µA cm^{-2} ($CR = 2.449$ mm y^{-1}) to 8.14 µA cm^{-2} ($CR = 0.095$ mm y^{-1}) at 50 °C. As expected, the corrosion rate is greater at higher temperature. On the other hand, in aerated solution high inhibition efficiency ($I_{corr} = 0.27$ µA cm^{-2}, $CR = 0.003$ mm y^{-1}) was reported at only the temperature of 50 °C. This was attributed to less oxygen being available at elevated temperatures. Adsorption studies showed that in a CO_2 environment a Freundlich isotherm gave the best fit for surface coverage data obtained at 25 °C, while a Langmuir isotherm best explained the surface coverage at 50 °C. In contrast, the surface coverage data obtained from aerated solutions at both 25 and 50 °C fitted well with the Langmuir adsorption isotherm. Calculation of Gibbs free energy of adsorption in CO_2-saturated brine solution ($\Delta G_{25\ °C} = -12.37$ kJ mol^{-1}, and $\Delta G_{50\ °C} = -15.55$ kJ mol^{-1}) indicated adsorption of inhibitor molecules was spontaneous and via physisorption[55].

Sida acuta

Aribo et al.[58] investigated the extract of *sida acuta* as a corrosion inhibitor for API 5L-X65 immersed in CO_2-saturated 3.5% NaCl solution. The experiments were conducted at 25 °C and in the presence of sand deposits. The authors evaluated the inhibitor performance at four different concentrations, 100, 200, 300 and 400 ppm[58].

Phytochemical analysis indicated the presence of alkaloid, flavonoid, phenol, saponin and tannins in the extract. Conclusions drawn from polarisation curves indicated that the inhibitive effect was more pronounced at higher concentrations of 300 and 400 ppm, and although there was not a significant corrosion rate reduction in the solution containing 100 ppm of inhibitor, there was still a suppression of the cathodic reaction. The corrosion potential at tested concentrations was found to shift to nobler potentials of more than 85 mV. Hence, the chemical mixture was classified as anodic inhibitor. The corrosion rate was found to decrease from 1.162 mm y^{-1} in uninhibited solution to 0.112 mm y^{-1} in solution containing 400 ppm of plant extract. This translated into an inhibition efficiency of 90%. The authors used AFM to study the surface morphology; however, they have not mentioned whether the 3D micrographs were obtained in situ or ex situ. The 3D micrographs showed a steel sample immersed in an uninhibited solution having a coarse and rough surface consistent with anodic dissolution. On the other hand, a sample immersed in inhibited solution had a smoother surface. Comparison of FTIR spectra obtained after removing the sample from the inhibited solution revealed the presence of amine functional groups on the sample surface confirming the presence of a nitrogen rich extract. Surface coverage data at different concentrations was found to best fit the Freundlich isotherm, which was attributed to the adsorption of inhibitor molecules being a non-ideal and reversible process, and that adsorption was not limited to monolayer formation[58].

Coptis chinensis and berberine

Zhao et al.[53] first studied the inhibition behaviour of berberine and *coptis chinensis* extract individually and then together with a synergist, thiourea[63]. The experiments were conducted on L360 carbon steel immersed in CO_2-saturated 3% NaCl solution and at 60 °C. Berberine was tested in three different concentrations (10, 50 and 100 ppm). *Coptis chinensis* was also tested in three different concentrations (10, 30 and 50 ppm)[53].

Coptis chinensis, a perennial stemless herb, is known to consist of alkaloids among which berberine, coptisine, epiberberine, magnoflorine and palmatine are considered to be the active compounds. Polarisation curves showed that the individual inhibitors provided only moderate corrosion inhibition. No significant shifts in corrosion potential and reduction in corrosion current density were observed; hence, the inhibitors were identified as mixed-type inhibitors. Initial results also showed that inhibitive properties of *coptis chinensis* were slightly better than those of berberine. Polarisation curves obtained after the addition of 10 ppm of synergist, thiourea, illustrated that there were significant changes in both anodic and cathodic branches. The blend of thiourea and *coptis chinensis* was found to provide better inhibition than the mixture of berberine and thiourea. It was also observed that the corrosion current density decreased when the individual inhibitor concentration was increased. Maximum inhibition efficiency of 95% was reported for a concentration of 50 ppm *coptis chinensis* and 10 ppm thiourea mixture. The corrosion current at 60 °C was found to decrease from 229 µA cm^{-2} ($CR = 2.661$ mm y^{-1}) in uninhibited solution to 9.7 µA cm^{-2} ($CR = 0.113$ mm y^{-1}) in this mixture. Nyquist plots obtained at 60 °C in the absence of a synergist showed that impedance spectra were composed of a larger capacitive loop, an inductive loop and a smaller capacitive loop. The diameters of both capacitive loops increased as the inhibitor concentration increased. It was observed that the inductive loop disappeared after the addition of synergist. The authors attributed the disappearance of the inductive loop to the absence of a relaxation process associated with either inhibitor molecules or H^+ ions adsorbing on the specimen surface. They concluded that the corrosion process was completely under charge transfer control after the addition of synergist. Calculation of charge transfer

resistance and double-layer capacitance showed that a mixture of thiourea and *coptis chinensis* provided better inhibition compared to a mixture of berberine and thiourea. In the case of a 50 ppm *coptis chinensis* and 10 ppm thiourea mixture, charge transfer resistance at 60 °C increased from 58.2 Ω cm^2 in uninhibited solutions to 1640 Ω cm^2. A Langmuir adsorption isotherm was found to best fit the surface coverage data. The standard free energy for 100 ppm berberine and 10 ppm thiourea mixture was calculated as −35.38 kJ mol^{-1}, which indicated that adsorption of the mixture can be attributed to both physisorption and chemisorption. On the other hand, the free energy of adsorption for the mixture of 50 ppm *coptis chinensis* and 10 ppm thiourea was calculated as −41.24 kJ mol^{-1} indicating adsorption via chemisorption. A synergistic effect of two inhibitors can be characterised by calculating the synergism parameter, denoted by *s*. When the value of *s* is greater than 1 it indicates a synergistic effect; a value less than 1 indicates an antagonistic effect, while a value equal to 1 represents an absence of any interaction between two inhibitor compounds. The synergistic effect of thiourea was confirmed as the synergism parameter for all tested blends was calculated to be greater than 1[53].

Licorice

Bajelani and Fattah-alhosseini[51] used licorice extract as a potential green corrosion inhibitor for API 5L Grade B carbon steel immersed in CO_2-saturated brine solution at 1 atm. The brine solutions were prepared according to NACE 1D196 standard and contained 3.5% NaCl, 0.305% $CaCl_2$ and 0.186% $MgCl_2.6H_2O$. The authors investigated five inhibitor concentrations at 25 °C, i.e., 40, 200, 1000, 2000 and 3000 ppm[51].

It was reported that glycyrrhizic acid and glabridin are the two primary active constituents of the liquorice extract. The Tafel polarisation curves illustrated that the addition of inhibitor significantly displaced the corrosion potential towards noble direction. Hence, the inhibitor was identified as an anodic inhibitor. The corrosion current density was observed to gradually decrease and inhibition efficiency progressively increased as the concentration of inhibitor was increased. The corrosion current decreased from 55 μA cm^{-2} ($CR = 0.639$ mm y^{-1}) to 9.9 μA cm^{-2} ($CR = 0.115$ mm y^{-1}) corresponding to an inhibition efficiency of 82% at an inhibitor concentration of 3000 ppm. Impedance measurement results plotted as Nyquist and Bode plots showed that the addition of inhibitor increased the charge transfer resistance of the system, corresponding to larger diameter capacitive loops. Inhibition efficiency values from impedance plots were in good agreement with those obtained from potentiodynamic polarisation curves. The experimental surface coverage data were found to fit a Langmuir adsorption isotherm. Calculation of Gibbs free energy indicated that inhibitor molecules spontaneously adsorb on the metal surface via physisorption[51].

Tobacco leaf

Kurniawan et al.[49] tested tobacco leaf extract as an organic inhibitor for AISI 1045 steel in CO_2-saturated 3.5% NaCl solution, at pH 4 and pH 7, and under dynamic conditions. The pH was adjusted using 1 M sodium bicarbonate ($NaHCO_3$) solution. The inhibitor was evaluated at three different concentrations, 132.5, 265 and 397.5 ppm and at two different rotational speeds, 150 and 250 rpm, using cylindrical electrodes with an area of 3.55 cm^2 [49].

Nicotine was identified as the main component of tobacco leaf extract. The weight loss method showed that 132.5 ppm of inhibitor resulted in a low corrosion rate of 0.091 mm y^{-1} at a lower rotational speed of 150 rpm and pH 7. On the other hand, at pH 4 a slightly higher concentration of inhibitor, 265 ppm, resulted in the lowest corrosion rate of 0.327 mm y^{-1}. Potentiodynamic polarisation results showed that the corrosion rate decreased from 1.774 to 0.244 mm y^{-1} when using 265 ppm of inhibitor at pH 4. Similarly, the corrosion rate decreased from 0.330 to 0.121 mm y^{-1} when using 132.5 ppm of inhibitor at pH 7. This corresponded to a maximum inhibitor efficiency of 63% at pH 7 and 86% at pH 4. The authors used the Tafel curves to characterise the inhibitor as a cathodic inhibitor. EIS results also showed that the addition of inhibitor increased the charge transfer resistance from 0.99 Ω (3.52 Ω cm^2) to 1.11 Ω (3.94 Ω cm^2) upon the addition of 265 ppm of inhibitor at pH 4. Similarly, the charge transfer resistance increased from 1.01 Ω (3.56 Ω cm^2) to 1.78 Ω (6.32 Ω cm^2) upon the addition of 132.5 ppm of inhibitor at pH 7. FTIR measurements, after removal of the test specimen from solution and drying, showed that inhibitor was still present on the steel surface. Investigation of the interaction mechanism showed that a Langmuir adsorption isotherm was best suited to fit the experimental data. The calculation of Gibbs free energy indicated that adsorption of inhibitor molecules on the substrate was spontaneous and the mode of adsorption was identified as physisorption[49].

Pomelo

Sun et al.[48] researched the effect of the addition of pomelo peel extract on the corrosion behaviour of N80 carbon steel in CO_2-saturated 3.5% NaCl solution. Several concentrations of the inhibitor were tested ranging from 0.1 to 0.4 g L^{-1} (100–400 ppm) at four different temperatures (30, 40, 50 and 60 °C) at pH 4.2[48].

Pomelo is a large citrus fruit and pomelo peel extract is known to be composed of flavonoids, coumarins and limonoids. The main component of pomelo peel extract was identified as naringin and used for quantum chemical calculations. Initially, weight loss measurements were used to calculate the corrosion rate and inhibition efficiency. It was found the inhibitor lowered the corrosion rate as its concentration was increased. However, an increase in temperature from 30 to 60 °C was found to lower the inhibition efficiency. This was attributed to the desorption of physically adsorbed inhibitor molecules. Polarisation curves showed that the corrosion current density decreased as the inhibitor concentration was increased. The polarisation results showed that the change in corrosion potential was less than 85 mV with the addition of inhibitor; hence, the inhibitor was identified as a mixed-type inhibitor. At 30 °C the corrosion current dropped from 158.81 μA cm^{-2} ($CR = 1.845$ mm y^{-1}) to 10.63 μA cm^{-2} ($CR = 0.124$ mm y^{-1}) for the solution with 400 ppm of inhibitor and indicated an inhibition efficiency of 93%. EIS analysis was conducted to obtain Nyquist and Bode plots. It was observed from Nyquist plots that an increase in inhibitor concentration resulted in capacitive loops of larger diameter that indicated that the addition of inhibitor increased the charge transfer resistance. Bode plots illustrated an increase in impedance slope and phase angle peaks that correspond to decreasing surface roughness as inhibitor concentration increased. Surface current values obtained from SECM analysis were smaller for the sample immersed in inhibited solution compared to the values obtained for the sample immersed in an uninhibited solution. SEM images were obtained after 6 h of immersion in uninhibited and inhibited solutions. The sample immersed in uninhibited solution had a damaged and rough surface, while the inhibited sample exhibited a smoother surface. FTIR spectra obtained after immersing and removing the steel sample from inhibited solution confirmed the presence of active elements of pomelo peel on the steel surface. A Langmuir adsorption isotherm gave the best fit for the calculated surface coverage data. Quantum chemical calculations depicted that protonated naringin had a high tendency for adsorption. It had lower E_{HOMO} values indicating its tendency to donate electrons to vacant d-orbitals of the iron, and lower values of E_{LUMO} suggested its ease of accepting electrons from iron into its p-orbital[48].

Calotropis procera

Ibrahim et al.[54] showed *calotropis procera* leaf extract to be an effective inhibitor for mild steel in CO_2-saturated 3.5% NaCl solution. The effectiveness of this inhibitor was compared for five different concentrations (25, 50, 100, 150 and 200 ppm) over a range of temperatures between 25 and 70 °C when CO_2 was being added at a rate of 3 L h^{-1} [54].

The plant extract is reported to be composed of alkaloids, cellulose, carbonyls, flavonoids, long chain fatty acids, amides, proteins and saponins. Amongst these, calotropin, uscharin, voruscharin and 2-oxovoruscharin were identified as active components and used in simulation studies. Evaluation of this inhibitor included calculation of the corrosion rate from LPR measurements. It was observed that the corrosion rate decreased and inhibition efficiency increased as the inhibitor concentration was increased. However, an increase in temperature was found to enhance the corrosion rate. The addition of plant extract resulted in the reduction of both cathodic and anodic reactions, however, a slightly larger decrease in the anodic reaction was observed with a net shift to nobler potentials and reduced current density. The maximum inhibition efficiency calculated was 92% corresponding to a concentration of 200 ppm at 40 °C that translated to a drop in corrosion rate from 4.463 mm y^{-1} in blank solution to 0.325 mm y^{-1} in 200 ppm inhibitor solution at 40 °C. It was observed that at all temperatures, the difference in corrosion potential shift from the blank solution to various tested concentrations was less than 85 mV, and hence, the inhibitor was identified as a mixed-type inhibitor. The protectiveness imparted by this plant extract was also confirmed through EIS. For all temperatures, it was observed that an increase in inhibitor concentration lowered the double-layer capacitance and increased the charge transfer resistance values. At 40 °C charge transfer resistance was found to increase from 138.60 Ω cm^2 in blank solution to 1611 Ω cm^2 in 200 ppm inhibitor-containing solution. This was attributed to the formation of a protective film. Comparison of SEM images showed that the inhibited sample had a smoother morphology in contrast to the sample immersed in an uninhibited solution. FTIR spectra obtained after immersing and removing the steel specimen from inhibitor-containing solution showed that the active ingredients of plant extract were still present on the steel surface. The surface coverage data were found to follow the Langmuir adsorption isotherm, and the adsorption constant was found to decrease as temperature increased. The calculated Gibbs free energy of adsorption for the experiment conducted at 40 °C was –4.55 kJ mol^{-1} indicating spontaneous physisorption of inhibitor molecules. Quantum chemical calculations showed that voruscharin had the highest E_{HOMO}, and lowest energy gap (ΔE) amongst the active ingredients and thus made the major contribution towards inhibition[54].

Corn oil

Abbasov et al.[50] synthesised and tested surfactants based on corn oil as corrosion inhibitors for C1018 mild steel samples in CO_2-saturated 1% NaCl solution at 0.9 bar. The five surfactants tested were sodium, potassium, ammonium salt of SFA, monoethanolamine and diethanolamine SFA. The effect of four different temperatures (20, 30, 40 and 50 °C), and five different concentrations (10, 25, 50, 75 100 ppm) were noted in this research work. A mixture of distilled water and isopropyl alcohol in a ratio of 70:30 was used to prepare the inhibitor solutions[50]. The authors have not cited any exact reason for this, but it can be assumed that it aimed to enhance the solubility of surfactants.

The maximum efficiency for all surfactants was achieved at a concentration of 100 ppm, which was near to their critical micelle concentration. The weight loss results obtained at 50 °C showed that the addition of all five inhibitors reduced the weight loss of the steel specimen but inhibition efficiency of diethanolamine SFA surfactant was the greatest. The inhibition efficiency increased in the following order: potassium SFA < sodium SFA < ammonium SFA < monoethanolamine SFA < diethanolamine SFA. According to weight loss measurements, the addition of 100 ppm of diethanolamine SFA reduced the corrosion rate from 3.78 to 0.001 mm y^{-1} corresponding to an efficiency of 99.9%. The reported LPR curves for all five surfactants were obtained after 1 h of pre-corrosion at 50 °C. A similar trend to the weight loss measurements was observed with inhibitor efficiency increasing as the inhibitor concentration increased. Polarisation curves illustrated that the addition of surfactant molecules shifted both the anodic and cathodic branches towards lower current densities. Since the displacement between uninhibited and inhibited corrosion potential was less than 85 mV, the inhibitor was identified as a mixed-type inhibitor. The maximum decrease in corrosion current from 2100 µA cm^{-2} ($CR = 24.401$ mm y^{-1}) to 21 µA cm^{-2} ($CR = 0.244$ mm y^{-1}) was noted for diethanolamine SFA that also translated to an inhibition efficiency of 99% at 100 ppm concentration. This was attributed to the increase in surface coverage of the substrate at a higher concentration. It was also concluded from Tafel curves that the overall corrosion kinetics of mild steel alloys in CO_2-saturated solutions were under anodic control. It is worth mentioning that the uninhibited and inhibited corrosion rates obtained from weight loss method and potentiodynamic polarisation vary greatly. This can be attributed to either the inherent differences between the techniques and/or a possible reporting or experimental error. SEM images clearly showed a damaged steel surface after immersion in uninhibited CO_2-saturated brine solution. In contrast, addition of 100 ppm of inhibitor resulted in a smooth surface protected by an inhibitor layer. The FTIR spectra obtained were used to confirm the formation of iron-sulfate fatty acid complex on the metal surface. A Langmuir adsorption isotherm best described the adsorption behaviour of surfactant molecules. Gibbs free energy higher than −40 kJ mol^{-1} indicated spontaneous adsorption of molecules via chemisorption. The concentration dependence of corrosion rate was attributed to the formation of multi-layers and increased surface coverage at higher inhibitor concentrations[50].

Dimocarpus longan

Priyotomo et al.[56] examined *dimocarpus longan* peel extract for its protective properties on API 5L steel immersed in CO_2-saturated brine. Inhibitor concentrations ranging from 50 to 700 ppm were evaluated at room temperature. The brine solution was prepared by mixing 12.874 g L^{-1} of NaCl, 7.374 g L^{-1} Na_2SO_4 and 0.912 g L^{-1} of $NaHCO_3$[56].

The literature identifies longan pericarp tissues to contain polyphenolic acids, flavonoids and polysaccharides[79]. Electrochemical parameters derived from polarisation curves illustrated that corrosion rate markedly decreased from 0.923 mm y^{-1} in uninhibited solution and attained the lowest value of 0.454 mm y^{-1} at a concentration of 400 ppm. There was no significant decrease in corrosion rate at higher concentrations. It was observed that the inhibition efficiency increased up to a concentration of 400 ppm but then decreased at higher concentrations. The maximum inhibition efficiency corresponding to 400 ppm was reported as 50%. Based on the observed shift in corrosion potential from uninhibited to inhibited states, the inhibitor was identified as mixed-type inhibitor. Impedance plots also showed that maximum charge transfer resistance was observed for a concentration of 400 ppm. The authors also suggested that the decrease in double-layer capacitance was due to the gradual replacement of water molecules by inhibitor molecules. Surface coverage data were found to obey Langmuir adsorption isotherm[56].

Gingko biloba

Singh et al.[57] studied the corrosion inhibition of N80 steel immersed in CO_2-saturated 3.5% NaCl solution using *gingko biloba* fruit extract. The investigated concentrations were 250, 500 and 1000 ppm. All experiments were conducted in stagnant solutions and at room temperature[57].

Mass spectrometry results revealed the presence of seven compounds in *gingko biloba* fruit extract. These identified compounds were D-galactose, 1-sec-butyldiaziridine, carbamic acid, 6-chlorohexanoic acid, 3-amino-4-pyrazolecarbonitrile, phenol, 3-pentadecyl and urea, N-methyl-N-nitroso. Since the difference in corrosion potential obtained from polarisation curves in uninhibited and inhibited states was less than 85 mV, the fruit extract was identified as a mixed-type inhibitor. The addition of inhibitor was found to shift both the anodic and cathodic branches towards lower current densities. The maximum shift was noted when the corrosion current dropped from 8.6 A cm^{-2} (8600 mA cm^{-2}) in an uninhibited state to 0.6 A cm^{-2} (600 mA cm^{-2}) upon addition of inhibitor to a concentration of 1000 ppm. It is worth noting here that since the authors have not cited a corrosion rate in mm y^{-1}, independent calculation of the corrosion rates using these corrosion current values appears to be exorbitantly high and the possibility of a reporting error cannot be eliminated. It was evident from EIS curves that charge transfer resistance increased as the concentration of the inhibitor increased. The maximum increase from 271 Ω cm^2 in the uninhibited state to 3869 Ω cm^2 was observed for a concentration of 1000 ppm, which corresponded to an inhibition efficiency of 92%. This was ascribed to the increased substrate surface coverage at higher concentration. The reported charge transfer resistances from EIS measurements also indicate an error in reporting the corrosion currents. Hence, this corrosion inhibitor is not summarised in Table 2. The 3D images from SECM measurements highlighted the contrast in tip current. Higher tip current was obtained when the probe passed over a steel surface immersed in uninhibited solution compared with sample surface areas immersed in inhibited solution. This was attributed to the formation of an insulating inhibitor layer on the steel surface. SEM images also supported the conclusion that a protective inhibitor layer was formed in inhibited solutions. The steel surface immersed in uninhibited solutions had a cracked and rough morphology while the samples immersed in inhibited solution exhibited a smoother and less corroded surface. A Temkin adsorption isotherm was found to give the best fit to describe the adsorption of inhibitor molecules at different concentrations that corresponded to varying surface coverage. However, thermodynamic parameters were not calculated and, therefore, no conclusions were made regarding the adsorption mechanism[57].

Momordica charantia

Singh et al.[46] investigated *momordica charantia* seed extract as an eco-friendly inhibitor for P110SS steel exposed to CO_2-saturated 3.5% NaCl solution. The effect of three concentrations (250, 500 and 1000 ppm) was tested at room temperature[46].

The authors listed cucurbitacin B, and momordicin I and II as the main biologically active compounds. The plant is also known to contain cytotoxic proteins (momorcharin and momordin), glycosides (charantin, charantosides, goyaglycosides, momordin and momordicosides) and terpenoids (momordol, momordenol, momordicilin, momordicinin and momordicinin-28). Tafel polarisation plots showed that since the addition of plant extract did not alter the corrosion potential more than 85 mV compared to the potential in uninhibited solution, the inhibitor behaves like a mixed-type inhibitor. An increase in inhibitor concentration resulted in lowering of the corrosion current density from 9.82 A cm^{-2} (9820 mA cm^{-2}) in blank solution to 1.01 A cm^{-2} (1010 mA cm^{-2}) in a solution containing 1000 ppm of the plant extract. Again, it is worth noting here that these corrosion current values appear to be exorbitantly high and are inconsistent with the charge transfer resistance measurements. It is therefore likely that this is a reporting error. The impedance measurement results illustrated that increase in inhibitor concentration resulted in increased charge transfer resistance from 154 Ω cm^2 in blank solutions to 3036 Ω cm^2 in 1000 ppm inhibitor-containing solution. The 3D plots obtained from SECM analysis confirmed that an insulating layer was formed on the metal surface when the specimen was immersed in the inhibited solution. A Langmuir adsorption isotherm gave the closest fit of the surface coverage data. The authors concluded that either the synergism between constituents of the green inhibitor extract was responsible for its good inhibition tendency or large-sized glycosides covering the specimen surface thereby providing corrosion resistance[46]. It is pointed out that because stainless steel generally undergoes localised corrosion and not general corrosion, and since LPR and EIS measure only a general or uniform corrosion rate, this inhibitor is not summarised in Table 2.

SUMMARY OF GREEN INHIBITORS FOR CO_2-SATURATED CORROSIVE MEDIA

The performance of the aforementioned green corrosion inhibitors for CO_2 corrosion is summarised in Table 2. Corrosion engineers generally require an inhibition rate of <0.1 mm y^{-1}. It can be seen in Table 2 that in many cases this target rate has been achieved. In the case of corn oil-derived diethanolamine SFA, the uninhibited corrosion rate of 24.01 mm y^{-1} appears quite excessive for the conditions stipulated.

In instances where the uninhibited and inhibited corrosion rates were not mentioned by authors[46,48,51,53,57,58], the following formula was used to determine the corrosion rates:

$$CR = ((I_{corr} * E_w)/\rho) * C \quad (10)$$

where CR is the corrosion rate in mm y^{-1}, I_{corr} is the current density in μA cm^{-2}, E_w is the equivalent weight of iron (E_w = 27.93 g/equivalent), ρ is the density ($\rho = 7.86$ g cm^{-3}) and C is the constant of proportionality ($C = 3.27 \times 10^{-3}$ when I_{corr} is in μA cm^{-2} and ρ is in g cm^{-3}).

GREEN INHIBITORS FOR CARBON STEEL IN ACIDIC MEDIA

Hot acidic solutions are typically utilised in oil well stimulation and induce severe corrosion attack on metallic components. Hence, many researchers have extensively worked with several different plant extracts in simulated hydrochloric and sulfuric acid environments. The earliest use (1973–2008) of such green inhibitors in acidic media is concisely presented in another review[80]. In the last couple of years (2016–2018), extracts from *glycyrrhiza glabra* leaf[59], sunflower seed hull[81], *pisum sativum* peel[67], *ginkgo biloba* leaf[65], cocoa bark[82], *aquilaria subintegra* leaf[83], longan peel[69], *griffonia simplicifolia* seed[84], *gentiana olivieri*[85], maple[60], *pennisetum purpureum* grass[86], *phyllanthus amarus* leaf[70] and *plantago ovata*[61] have been evaluated for their corrosion inhibiting potential in hydrochloric solutions of varying concentrations. Similarly, many plant extracts have been studied as green corrosion inhibitors for mild steel in sulfuric acid solutions of different concentrations. Contemporary research (2016–2018), for example, has dealt with extracts from loquat leaf[87], *sida cordifolia*[66] and *aster koraiensis* leaf[88]. It is imperative to state that the authors who worked with *sida cordifolia* reported the corrosion rate for mild steel in blank, 0.5 M sulfuric acid as 0.000104 mm y^{-1}[66]. This obviously appears very low and erroneous; hence, it is emphasised that results from such works are corroborated. Preceding works, from 1982 to 2015, on plant extracts as green corrosion inhibitors for steel in sulfuric acid are compiled in a separate review[89]. Results from research were extracted and the performance of green inhibitors was compiled

Table 3. Green corrosion inhibitors for preventing corrosion in hydrochloric acid solution sorted based on the lowest corrosion rate obtained from polarisation parameters.

Plant extract	Steel specimen	Inhibitor concentration (at max. IE%)	Testing temperature (°C)	Uninhibited corrosion rate (mm y^{-1})	Inhibited corrosion rate (mm y^{-1})	Testing solution
Sunflower seed hull	MS	400 ppm	25	3.509	0.054	1.0 M HCl
Maple	A1010 LCS	0.4 g/L (400 ppm)	25	1.836	0.116	1.0 M HCl
Cocoa bark	A1020 LCS	1.112 g/L (1112 ppm)	30	1.162	0.128	18.23 g/L HCl (0.5 M HCl)
Griffonia simplicifolia seed	MS	1000 ppm	30	11.263	0.163	1.0 M HCl
Maple	A1010 LCS	0.4 g/L (400 ppm)	25	1.140	0.163	1.0 M HCl
Pisum sativum peel	MS	0.4 g/L (400 ppm)	30	2.754	0.349	1.0 M HCl
Gentiana olivieri	MS	800 mg/L (800 ppm)	20	3.509	0.349	0.5 M HCl
Longan peel	MS	600 mg/L (600 ppm)	25	4.934	0.349	0.5 M HCl
Aquilaria subintegra leaf	MS	1500 ppm	30	3.277	0.372	1.0 M HCl
Ginkgo biloba leaf	X70	200 mg/L (200 ppm)	30	4.047	0.403	1.0 M HCl
Glycyrrhiza glabra leaf	MS	800 ppm	25	3.026	0.467	1.0 M HCl
Griffonia simplicifolia seed	J55	1000 ppm	30	7.145	0.482	1.0 M HCl
Griffonia simplicifolia seed	X80	1000 ppm	30	8.061	0.578	1.0 M HCl
Phyllanthus amarus leaf	MS	4 v/v % (40,000 ppm)	30	12.270	0.593	1.0 M HCl
Pennisetum purpureum grass	MS	5.0 g/L + 0.1 mol/L KI (5000 ppm + 16,600 ppm KI)	30	16.153	0.634	3.5% HCl (1.0 M HCl)
Ginkgo biloba leaf	X70	200 mg/L (200 ppm)	30	8.399	0.727	1.0 M HCl
Plantago ovata	A1020 LCS	1000 ppm	30	14.042	1.050	1.0 M HCl
Ginkgo biloba leaf	X70	200 mg/L (200 ppm)	30	14.432	1.125	1.0 M HCl
Phyllanthus amarus leaf	MS	4 v/v % (40,000 ppm)	30	40.111	1.871	1.0 M HCl
Phyllanthus amarus leaf	MS	4 v/v % (40,000 ppm)	30	42.052	14.908	1.0 M HCl

MS mild steel, *LCS* low carbon steel, *IE* inhibition efficiency.

Table 4. Green corrosion inhibitors for preventing corrosion in sulfuric acid solution sorted based on the lowest corrosion rate obtained from polarisation parameters.

Plant extract	Steel specimen	Inhibitor concentration (at max. IE%)	Testing temperature (°C)	Uninhibited corrosion rate (mm y^{-1})	Inhibited corrosion rate (mm y^{-1})	Testing solution
Loquat leaf	MS	100 v/v% (1,000,000 ppm)	30	6.716	0.244	0.5 M H_2SO_4
Aster koraiensis leaf	MS	2000 ppm	30	7.739	1.220	1.0 M H_2SO_4

MS mild steel, *IE* inhibition efficiency.

as shown in Tables 3 and 4 for hydrochloric and sulfuric acid, respectively.

It is essential here to mention the inconsistencies between the reported corrosion rates in blank solutions. In the case of strong acid conditions (Table 3) a targeted corrosion rate of 0.1 mm y^{-1} or less was not achieved in many cases. Further work is required to investigate synergistic effects and with other plant extracts to reach this target rate.

It can be seen from Table 3 that the corrosion rates for mild steel in blank, 1.0 M hydrochloric acid solutions for temperatures 20–40 °C vary greatly from 2.754 mm y^{-1} to an astonishing 42.052 mm y^{-1}. In addition, it can also be observed from Table 3 that authors who worked with Maple leaf extract reported a lower corrosion rate at a higher temperature for the same metal specimen, A1010 LCS. One would expect the corrosion rate at the higher temperature to be significantly much higher and not less. It is stressed here that these variations in the reported results can only partly be attributed to the differences in steel specimen, and the possibility of reporting errors, human or experimental errors cannot be eliminated.

It is worthwhile to study and compare the performance of inhibitors used in hydrochloric and sulfuric acid media as potential green inhibitors for CO_2-saturated saline environments as well. It is possible that an inhibitor can perform equally well or maybe better in sweet corrosive conditions.

CONCLUSIONS AND FUTURE PROSPECTS

In large pipelines corrosion inhibitors remain the primary means of combating internal corrosion concomitant with oil and gas

production and transportation. Conventional corrosion inhibitors can be toxic and the disposal of unused inhibitor concentrates has driven many researchers to study and develop environmentally friendly alternatives. The development and practical use of such green inhibitors is subject to the fact that new inhibitor formulations have to conform to various regulations while upholding similar inhibitor efficiencies as conventional industrial inhibitors. Rigorous protocols dictate that an ideal green inhibitor is non-toxic, biodegradable and shows no bioaccumulation. In light of this definition, many researchers have exploited the biodegradable nature of plant extracts and evaluated the performance of plant-extract-based inhibitors using various laboratory techniques.

As has been demonstrated in this review, high concentrations of plant-extract-based inhibitors are sometimes required to provide similar levels of protection as conventional inhibitors. Although the majority of the plant-extract-based inhibitors provide adequate levels of protection, there is still a need to optimise such formulations. One such way of optimisation is by conducting phytochemical screening and performing quantum chemical and molecular dynamic simulations to identify the most active ingredient of the various phytochemicals present in a plant extract. The next step of such optimisation is studying the synergism between these active molecules to create an overall superior formulation. Most of the commercial inhibitor formulations are also typically a blend of different chemical compounds.

The performance of plant extracts, as corrosion inhibitors, has mostly been investigated under atmospheric conditions using basic electrochemical techniques. In some cases, the reported corrosion rates in blank solutions of similar corrosivity vary greatly to the extent that is difficult to attribute them merely to changes in reaction kinetics associated with variations in elemental composition and microstructure of the carbon steels. This suggests probable laboratory errors in obtaining the corrosion rates.

Oil and gas are produced under conditions of high pressure and temperature where the partial pressure of corrosive gases like CO_2 can substantially exceed 1 bar. Therefore, for oil and gas field applications more stringent laboratory tests need to be conducted at high pressure, high temperature and shear stress. These include jet impingement, rotating cage and RCE tests in autoclaves. In addition, researchers have assessed plant-extract-based inhibitors in only water-based electrolytes. Therefore, future research also needs to analyse the performance of such inhibitors in oil–water or condensate–water mixtures. This type of research direction could be further extended by including impurities like sludge or sand to determine the ability of such materials to adsorb on active inhibitor ingredients and render the plant-extract-based green material less effective. This approach is often taken in commercial corrosion inhibitor evaluations.

In short, there is an urgent need of suitable green inhibitors given the extensive use of mild steel and the resulting economical loss in the form of corrosion. The development of an adequate and commercial plant-extract-based green inhibitor suitable for trialling in oil and gas fields appears to be a practically beneficial research area with great potential for innovation in inhibitor formulations.

Received: 31 March 2021; Accepted: 13 July 2021;
Published online: 25 January 2022

REFERENCES

1. Tiu, B. D. B. & Advincula, R. C. Polymeric corrosion inhibitors for the oil and gas industry: design principles and mechanism. *React. Funct. Polym.* **95**, 25–45 (2015).
2. Usman, B. J. & Ali, S. A. Carbon dioxide corrosion inhibitors: a review. *Arab J. Sci. Eng.* **43**, 1–22 (2018).
3. Javidi, M. & Bekhrad, S. Failure analysis of a wet gas pipeline due to localised CO_2 corrosion. *Eng. Fail. Anal.* **89**, 46–56 (2018).
4. Paolinelli, L. D., Pérez, T. & Simison, S. N. The effect of pre-corrosion and steel microstructure on inhibitor performance in CO_2 corrosion. *Corros. Sci.* **50**, 2456–2464 (2008).
5. Nešić, S. Carbon dioxide corrosion of mild steel. In *Uhlig's Corrosion Handbook* (ed. Revie, R. W.) 229–245 (John Wiley & Sons, Inc., 2011). https://doi.org/10.1002/9780470872864.ch19.
6. Remita, E. et al. Hydrogen evolution in aqueous solutions containing dissolved CO_2: quantitative contribution of the buffering effect. *Corros. Sci.* **50**, 1433–1440 (2008).
7. Tran, T., Brown, S., & Nesić, S. *Corrosion of Mild Steel in an Aqueous CO_2 Environment – Basic Electrochemical Mechanisms Revisited* (NACE International, 2015).
8. Dugstad, A. *Fundamental Aspects of CO_2 Metal Loss Corrosion – Part 1: Mechanism* (NACE International, 2006).
9. Nesić, S., Postlethwaite, J. & Vrhovac, M. CO_2 corrosion of carbon steel – from mechanistic to empirical modelling. *Corros. Rev.* **15**, 211–240 (1997).
10. Nešić, S. Key issues related to modelling of internal corrosion of oil and gas pipelines – a review. *Corros. Sci.* **49**, 4308–4338 (2007).
11. Carroll, J. J., Slupsky, J. D. & Mather, A. E. The solubility of carbon dioxide in water at low pressure. *J. Phys. Chem. Ref. Data* **20**, 1201–1209 (1991).
12. Crovetto, R. Evaluation of solubility data of the system CO_2 –H_2O from 273 K to the critical point of water. *J. Phys. Chem. Ref. Data* **20**, 575–589 (1991).
13. Bockris, J. O., Drazic, D. & Despic, A. R. The electrode kinetics of the deposition and dissolution of iron. *Electrochim. Acta* **4**, 325–361 (1961).
14. Bénézeth, P., Dandurand, J. L. & Harrichoury, J. C. Solubility product of siderite ($FeCO_3$) as a function of temperature (25–250 °C). *Chem. Geol.* **265**, 3–12 (2009).
15. Sun, W., Nešić, S. & Woollam, R. C. The effect of temperature and ionic strength on iron carbonate ($FeCO_3$) solubility limit. *Corros. Sci.* **51**, 1273–1276 (2009).
16. Dugstad, A. & Seiersten, M. *pH-Stabilisation, A Reliable Method for Corrosion Control of Wet Gas Pipelines* (Society of Petroleum Engineers, 2004).
17. Pandarinathan, V., Lepková, K. & van Bronswijk, W. Chukanovite ($Fe_2(OH)_2CO_3$) identified as a corrosion product at sand-deposited carbon steel in CO_2-saturated brine. *Corros. Sci.* **85**, 26–32 (2014).
18. Vanaei, H. R., Eslami, A. & Egbewande, A. A review on pipeline corrosion, in-line inspection (ILI), and corrosion growth rate models. *Int. J. Press. Vessels Pip.* **149**, 43–54 (2017).
19. Hou, Y., Aldrich, C., Lepkova, K. & Kinsella, B. Detection of under deposit corrosion in a CO_2 environment by using electrochemical noise and recurrence quantification analysis. *Electrochim. Acta* **274**, 160–169 (2018).
20. Xu, M. et al. Effect of pressure on corrosion behavior of X60, X65, X70, and X80 carbon steels in water-unsaturated supercritical CO_2 environments. *Int. J. Greenh. Gas. Control* **51**, 357–368 (2016).
21. Sui, P. et al. Effect of temperature and pressure on corrosion behavior of X65 carbon steel in water-saturated CO_2 transport environments mixed with H_2S. *Int. J. Greenh. Gas. Control* **73**, 60–69 (2018).
22. Sparr, M. & Kimab, S. *Influence of Test Conditions and Test Methods in the Evaluation of Corrosion Inhibitors Used In Pipelines – A Review* (NACE International, 2011).
23. Singh, W. P. & Bockris, J. O. *Toxicity Issues of Organic Corrosion Inhibitors: Applications of QSAR Model* (NACE International, 1996).
24. Singh, A. K. & Quraishi, M. A. Effect of Cefazolin on the corrosion of mild steel in HCl solution. *Corros. Sci.* **52**, 152–160 (2010).
25. Durnie, W. H., Kinsella, B. J., Marco, R. D. & Jefferson, A. A study of the adsorption properties of commercial carbon dioxide corrosion inhibitor formulations. *J. Appl. Electrochem* **31**, 1221–1226 (2001).
26. Durnie, W., DE Marco, R., Kinsella, B., Jefferson, A. & Pejcic, B. Predicting the adsorption properties of carbon dioxide corrosion inhibitors using a structure-activity relationship. *J. Electrochem. Soc.* **152**, B1 (2005).
27. Durnie, W. H., De Marco, R., Jefferson, A. & Kinsella, B. J. In situ SERS study of the adsorption of inhibitors of carbon dioxide corrosion. *Surf. Interface Anal.* **35**, 536–543 (2003).
28. Bahlakeh, G., Ramezanzadeh, M. & Ramezanzadeh, B. Experimental and theoretical studies of the synergistic inhibition effects between the plant leaves extract (PLE) and zinc salt (ZS) in corrosion control of carbon steel in chloride solution. *J. Mol. Liq.* **248**, 854–870 (2017).
29. Rajendran, S., Shanmugapriya, S., Rajalakshmi, T. & Amal Raj, A. J. Corrosion inhibition by an aqueous extract of rhizome powder. *CORROSION* **61**, 685–692 (2005).
30. Eddy, N. O., Odoemelam, S. A. & Odiongenyi, A. O. Joint effect of halides and ethanol extract of Lasianthera africana on inhibition of corrosion of mild steel in H_2SO_4. *J. Appl. Electrochem.* **39**, 849–857 (2009).
31. Rahim, A. A. et al. Mangrove tannins and their flavanoid monomers as alternative steel corrosion inhibitors in acidic medium. *Corros. Sci.* **49**, 402–417 (2007).

32. Bouyanzer, A., Hammouti, B. & Majidi, L. Pennyroyal oil from Mentha pulegium as corrosion inhibitor for steel in 1M HCl. *Mater. Lett.* **60**, 2840–2843 (2006).
33. Oguzie, E. E. et al. Characterization and experimental and computational assessment of *Kola nitida* extract for corrosion inhibiting efficacy. *Ind. Eng. Chem. Res.* **53**, 5886–5894 (2014).
34. Oguzie, E. E. et al. Natural products for materials protection: mechanism of corrosion inhibition of mild steel by acid extracts of *Piper guineense*. *J. Phys. Chem. C.* **116**, 13603–13615 (2012).
35. Rybolt, T. R. & Hansel, R. A. Determining molecule–carbon surface adsorption energies using molecular mechanics and graphene nanostructures. *J. Colloid Interface Sci.* **300**, 805–808 (2006).
36. Taj, S. Papavinasam, S. & Revie, R. W. *Development of Green Inhibitors for Oil and Gas Applications*. (NACE International, 2006).
37. Papavinasam, S. *Corrosion Control in the Oil and Gas Industry* (Elsevier, 2013).
38. Loto, C. A. Electrochemical noise measurement technique in corrosion research. *Int J. Electrochem Sci.* **7**, 9248–9270 (2012).
39. Tan, Y. J., Bailey, S. & Kinsella, B. The monitoring of the formation and destruction of corrosion inhibitor films using electrochemical noise analysis (ENA). *Corros. Sci.* **38**, 1681–1695 (1996).
40. Hou, Y., Aldrich, C., Lepkova, K., Machuca, L. L. & Kinsella, B. Monitoring of carbon steel corrosion by use of electrochemical noise and recurrence quantification analysis. *Corros. Sci.* **112**, 63–72 (2016).
41. Hou, Y., Aldrich, C., Lepkova, K. & Kinsella, B. Identifying corrosion of carbon steel buried in iron ore and coal cargoes based on recurrence quantification analysis of electrochemical noise. *Electrochim. Acta* **283**, 212–220 (2018).
42. Ferreira, E. S., Giacomelli, C., Giacomelli, F. C. & Spinelli, A. Evaluation of the inhibitor effect of l-ascorbic acid on the corrosion of mild steel. *Mater. Chem. Phys.* **83**, 129–134 (2004).
43. Nathan, C. C. (ed.) *Corrosion Inhibitors* (National Association of Corrosion Engineers, 1994).
44. D, A. O. Langmuir, Freundlich, Temkin and Dubinin–Radushkevich isotherms studies of equilibrium sorption of Zn^{2+} unto phosphoric acid modified rice husk. *IOSR J. Appl. Chem.* **3**, 38–45 (2012).
45. Abeng, F. E., Idim, V. D., Obono, O. E. & Magu, T. O. Adsorption and adsorption isotherm: application to corrosion inhibition studies of mild steel in 2 M HCl. *World Sci. N.* **77**, 298–313 (2017).
46. Singh, A., Lin, Y., Liu, W., Ebenso, E. E. & Pan, J. Extract of *Momordica charantia* (Karela) seeds as corrosion inhibitor for P110SS steel in CO_2 saturated 3.5% NaCl solution. *Int J. Electrochem Sci.* **8**, 12884–12893 (2013).
47. Chen, S. et al. Inhibition effect of ilex kudingcha C.J. Tseng (kudingcha) extract on J55 steel in 3.5wt% NaCl solution saturated with CO_2. *Int J. Electrochem Sci.* **12**, 782–796 (2017).
48. Sun, Z. et al. Inhibition effect of pomelo peel extract for N80 steel in 3.5% NaCl saturated with CO_2 solution. *Res. Chem. Intermed.* **43**, 6719–6736 (2017).
49. Kurniawan, B. A., Pratiwi, V. M. & Ahmadi, N. F. Effect of fluid flow, pH and tobacco extracts concentration as organic inhibitors to corrosion characteristics of AISI 1045 steel in 3.5% NaCl environment containing CO_2 gas. *AIP Conf. Proc.* **1945**, 020050 (2018).
50. Abbasov, V. M. et al. A study of the corrosion inhibition of mild steel C1018 in CO_2-saturated brine using some novel surfactants based on corn oil. *Egypt J. Pet.* **22**, 451–470 (2013).
51. Bajelani, A. & Fattah-alhosseini, A. Inhibition of API 5L Gr.B carbon steel corrosion using licorice extract in CO_2 environment. *Anal. Bioanal. Electrochem.* **8**, 409–422 (2016).
52. Aribo, S., Olusegun, S. J., Ibhadiyi, L. J., Oyetunji, A. & Folorunso, D. O. Green inhibitors for corrosion protection in acidizing oilfield environment. *J. Assoc. Arab Univ. Basic Appl. Sci.* **24**, 34–38 (2017).
53. Zhao, J., Duan, H. & Jiang, R. Synergistic corrosion inhibition effects of coptis extract/berberine and thiourea on the corrosion of mild steel in carbon dioxide saturated brine solution. *Int J. Electrochem Sci.* **10**, 24 (2015).
54. Ibrahim, T., Gomes, E., Obot, I. B., Khamis, M. & Abou Zour, M. Corrosion inhibition of mild steel by Calotropis procera leaves extract in a CO_2 saturated sodium chloride solution. *J. Adhes. Sci. Technol.* **30**, 2523–2543 (2016).
55. Aribo, S., Sanumi, O. J., Olusegun, S. J., Ogunbadejo, A. S. & Ige, O. O. Jatropha curcas as a corrosion inhibitor for API 5L-X65 steel under sand deposit in CO_2 and aerated oilfield environments. *Afr. Corr. J.* **2**, 17–27 (2016).
56. Priyotomo, G. A study on Dimocarpus longan peel as corrosion inhibitor on steel in artificial brine solutions. *Res. Dev. Mater. Sci.* **6**, 555–559 (2018).
57. Singh, A. et al. A study on the inhibition of N80 steel in 3.5% NaCl solution saturated with CO_2 by fruit extract of *Gingko biloba*. *J. Taiwan Inst. Chem. Eng.* **45**, 1918–1926 (2014).
58. Aribo, S. et al. Under-deposit corrosion behaviour of API 5L-X65 steel in CO_2 environment containing *Sida Acuta* extract. *Leonardo El J. Pr. Technol.* **16**, 265–274 (2017).
59. Alibakhshi, E. et al. *Glycyrrhiza glabra* leaves extract as a green corrosion inhibitor for mild steel in 1 M hydrochloric acid solution: experimental, molecular dynamics, Monte Carlo and quantum mechanics study. *J. Mol. Liq.* **255**, 185–198 (2018).
60. Jokar, M., Farahani, T. S. & Ramezanzadeh, B. Electrochemical and surface characterizations of morus alba pendula leaves extract (MAPLE) as a green corrosion inhibitor for steel in 1M HCl. *J. Taiwan Inst. Chem. Eng.* **63**, 436–452 (2016).
61. Mobin, M. & Rizvi, M. Polysaccharide from Plantago as a green corrosion inhibitor for carbon steel in 1M HCl solution. *Carbohydr. Polym.* **160**, 172–183 (2017).
62. Njoku, D. I., Li, Y., Lgaz, H. & Oguzie, E. E. Dispersive adsorption of *Xylopia aethiopica* constituents on carbon steel in acid-chloride medium: a combined experimental and theoretical approach. *J. Mol. Liq.* **249**, 371–388 (2018).
63. Njoku, D. I., Oguzie, E. E. & Li, Y. Characterization, electrochemical and theoretical study of the anticorrosion properties of *Moringa oleifera* extract. *J. Mol. Liq.* **237**, 247–256 (2017).
64. Pandarinathan, V., Lepková, K., Bailey, S. I., Becker, T. & Gubner, R. Adsorption of corrosion inhibitor 1-dodecylpyridinium chloride on carbon steel studied by in situ AFM and electrochemical methods. *Ind. Eng. Chem. Res.* **53**, 5858–5865 (2014).
65. Qiang, Y., Zhang, S., Tan, B. & Chen, S. Evaluation of Ginkgo leaf extract as an eco-friendly corrosion inhibitor of X70 steel in HCl solution. *Corros. Sci.* **133**, 6–16 (2018).
66. Saxena, A., Prasad, D., Haldhar, R., Singh, G. & Kumar, A. Use of Sida cordifolia extract as green corrosion inhibitor for mild steel in 0.5 M H_2SO_4. *J. Environ. Chem. Eng.* **6**, 694–700 (2018).
67. Srivastava, M. et al. Low cost aqueous extract of *Pisum sativum* peels for inhibition of mild steel corrosion. *J. Mol. Liq.* **254**, 357–368 (2018).
68. Pustaj, G., Kapor, F. & Jakovljević, S. Carbon dioxide corrosion of carbon steel and corrosion inhibition by natural olive leaf extract: Die Kohlendioxid-Korrosion von Kohlenstoffstahl und die Korrosionshemmung durch natürlichen Olivenblattextrakt. *Mater. Werkst.* **48**, 122–138 (2017).
69. Liao, L. L., Mo, S., Luo, H. Q. & Li, N. B. Longan seed and peel as environmentally friendly corrosion inhibitor for mild steel in acid solution: experimental and theoretical studies. *J. Colloid Interface Sci.* **499**, 110–119 (2017).
70. Anupama, K. K., Ramya, K. & Joseph, A. Electrochemical and computational aspects of surface interaction and corrosion inhibition of mild steel in hydrochloric acid by *Phyllanthus amarus* leaf extract (PAE). *J. Mol. Liq.* **216**, 146–155 (2016).
71. Ehsani, A. et al. Evaluation of *Thymus vulgaris* plant extract as an eco-friendly corrosion inhibitor for stainless steel 304 in acidic solution by means of electrochemical impedance spectroscopy, electrochemical noise analysis and density functional theory. *J. Colloid Interface Sci.* **490**, 444–451 (2017).
72. Ramezanzadeh, M., Sanaei, Z., Bahlakeh, G. & Ramezanzadeh, B. Highly effective inhibition of mild steel corrosion in 3.5% NaCl solution by green Nettle leaves extract and synergistic effect of eco-friendly cerium nitrate additive: experimental, MD simulation and QM investigations. *J. Mol. Liq.* **256**, 67–83 (2018).
73. Philip, J. Y. N., Buchweishaija, J. & Mkayula, L. L. Cashew nut shell liquid as an alternative corrosion inhibitor for carbon steels. *Tanz J. Sci.* **27**, 9–19 (2001).
74. Philip, J. Y. N., Buchweishaija, J. & Mkayula, L. L. Mechanistic studies of carbon steel corrosion inhibition by cashew nut shell liquid. *Tanz J. Sci.* **28**, 105–116 (2002).
75. Lee, O.-H. et al. Assessment of phenolics-enriched extract and fractions of olive leaves and their antioxidant activities. *Bioresour. Technol.* **100**, 6107–6113 (2009).
76. Hayes, J. E., Allen, P., Brunton, N., O'Grady, M. N. & Kerry, J. P. Phenolic composition and in vitro antioxidant capacity of four commercial phytochemical products: Olive leaf extract (*Olea europaea* L.), lutein, sesamol and ellagic acid. *Food Chem.* **126**, 948–955 (2011).
77. El-Etre, A. Y. Inhibition of acid corrosion of carbon steel using aqueous extract of olive leaves. *J. Colloid Interface Sci.* **314**, 578–583 (2007).
78. Mohadyaldinn, M. E. & Azad, N. A. A. K. Evaluation of *Jatropha Curcas* oil as corrosion inhibitor of CO_2 corrosion in petroleum production environment. *J. Appl. Environ. Biol. Sci.* **7**, 28–34 (2017).
79. Rangkadilok, N., Worasuttayangkurn, L., Bennett, R. N. & Satayavivad, J. Identification and quantification of polyphenolic compounds in longan (*Euphoria longana* Lam.) fruit. *J. Agric. Food Chem.* **53**, 1387–1392 (2005).
80. Buchweishaija, J. Phytochemicals as green corrosion inhibitors in various corrosive media: a review. *Tanz. J. Sci.* **35**, 77–92 (2009).
81. Hassannejad, H. & Nouri, A. Sunflower seed hull extract as a novel green corrosion inhibitor for mild steel in HCl solution. *J. Mol. Liq.* **254**, 377–382 (2018).
82. Barreto, L. S. et al. Study and assessment of the efficiency of the cocoa bark extracted from the Theobroma Cacao as an inhibitor of the corrosion of carbon steel in substitution of benzotriazole. *Mater. Res.* **21**, e20160309 (2018).
83. Sin, H. L. Y. et al. Aquilaria subintergra leaves extracts as sustainable mild steel corrosion inhibitors in HCl. *Measurement* **109**, 334–345 (2017).

84. Ituen, E., Akaranta, O., James, A. & Sun, S. Green and sustainable local biomaterials for oilfield chemicals: *Griffonia simplicifolia* extract as steel corrosion inhibitor in hydrochloric acid. *Sustain. Mater. Technol.* **11**, 12–18 (2017).
85. Baran, E., Cakir, A. & Yazici, B. Inhibitory effect of *Gentiana olivieri* extracts on the corrosion of mild steel in 0.5 M HCl: electrochemical and phytochemical evaluation. *Arab. J. Chem.* **12**, 4303–4319 (2019).
86. Ituen, E., James, A., Akaranta, O. & Sun, S. Eco-friendly corrosion inhibitor from *Pennisetum purpureum* biomass and synergistic intensifiers for mild steel. *Chin. J. Chem. Eng.* **24**, 1442–1447 (2016).
87. Zheng, X., Gong, M., Li, Q. & Guo, L. Corrosion inhibition of mild steel in sulfuric acid solution by loquat (*Eriobotrya japonica* Lindl.) leaves extract. *Sci. Rep.* **8**, 9140 (2018).
88. Prabakaran, M. et al. Aster koraiensis as nontoxic corrosion inhibitor for mild steel in sulfuric acid. *J. Ind. Eng. Chem.* **52**, 235–242 (2017).
89. Mo, S., Luo, H.-Q. & Li, N.-B. Plant extracts as "green" corrosion inhibitors for steel in sulphuric acid. *Chem. Pap.* **70**, 1131–1143 (2016).

ACKNOWLEDGEMENTS

B. R. F. would like to acknowledge the Australian Government Research Training Program (RTP) Scholarship in supporting this research.

AUTHOR CONTRIBUTIONS

All authors contributed to the discussions, directions and development of this review paper. B. R. F. primarily wrote the review manuscript. All co-authors reviewed and provided feedback to form the final version of this review paper.

COMPETING INTERESTS

The authors declare no competing interests.

ADDITIONAL INFORMATION

Correspondence and requests for materials should be addressed to Katerina Lepkova.